Comparative analysis of two antennas for communication in 2.4 GHz

Edgar Manuel Branco Ruano, *Military Academy, IST*

Abstract—The need for antennas for communication with unmanned systems used by the military to perform surveillance and recognition tasks led to the development of this work. This paper has the objective to design and build a prototype of an antenna, which is able to perform wireless communication between the operator and unmanned systems. The work was focused on the optimization and practical use of an ESPAR (Eletronically Steerable Passive Arrays Radiators) antenna, using the technique of genetic algorithms. This antenna allows a directional radiation pattern which can be switched in azimuth. Initially the antenna has been designed and simulated in 4NEC2X simulation program, to operate in the band of 2.4 GHz. The construction of a prototype involved also the construction of a basic structure and the inclusion of electronic components. After construction, the antenna was tested in an anechoic chamber and performed measurements of radiation patterns and the S_{11} parameter were performed. The measurement results confirmed the characteristics of directive radiation and the switch of the radiation pattern in azimuth, which is in accordance with the performed simulations. At the end realizes the comparison of ESPAR antenna built as part of this work, with a printed Yagi-Uda, whose prototype was carried out in a previous master's thesis.

***Keywords*—ESPAR antenna, Yagi-Uda antenna, Switched Parasitic Arrays (SPA), genetic algorithms**

I. INTRODUCTION

Nowadays the Armed Forces of the most developed countries have at their disposal the most innovative technologies. The development of these technologies allows, the domain of the OT (Operations Theatre) in case of conflict. For surveillance and recognition of the OT unmanned systems are increasingly used [1]. The Portuguese Army has developed robots for ground surveillance, which are part of a project denominated ROVIM (Robot Surveillance for Military Facilities). These robots perform wireless communications in band of 2.4 GHz, with an operator that is controlling them remotely. The robot has a steerable monopole type antenna, while the operator must have an antenna to communicate in the same frequency band. This antenna must have some features that are essential for using at a military level such as: robustness, small size and a directive radiation pattern that can be switched in azimuth.

The purpose of this thesis was to simulate, build and test an ESPAR antenna and finally, compare its performance with a printed Yagi-Uda smart antenna which was designed and built previously.

The practical component of this design is high, because the ESPAR antenna is composed of a basic structure with a complex geometry and includes electronic components to control the radiation pattern.

II. STATE OF THE ART

A. Antennas configuration

The Yagi-Uda antenna is composed by an active element (x_2), a dipole, and parasitic elements (x_1, x_3, x_4, x_5) aligned along the x-axis (Fig. 1) [2].

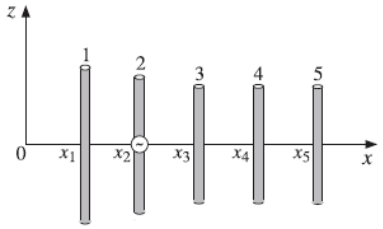

Fig. 1 – Scheme of the conventional Yagi-Uda [2]

The ESPAR antenna is composed by an active element (#0), a monopole, and by a ring of parasitic elements (#1, #2, #3, #4, #5) around the central element. According to the scheme of figure 2, it can be seen how the elements are arranged on the ground plane. Under the ground plane and the respective tab, the electronic components associated with the several parasitic elements are inserted.

Parasites monopole are disposed on the ground plane in the form of a regular polygon.

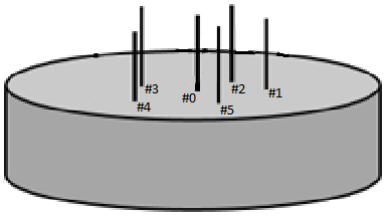

Fig. 2 – Scheme of the ESPAR 6 elements

B. Historic evolution

The development of wireless communications, has led to the study of antennas to operate in the 2.4 GHz frequency band. The need for antennas with high directivity and specific types of radiation patterns, contributed to the development of antennas arrays. The Yagi-Uda antenna was developed in the mid-1920. Initially it was applied to analogue TV reception. The first arrays were characterized by having a fixed radiation pattern, no digital processing, and the variation of the radiation pattern was achieved by changing the position of the antenna.

In the 1970s, there was a major breakthrough in antenna arrays, with the advent of smart antennas arrays with built-in digital processing [3].

In 1978, Roger F. Harrington developed the concept of parasitic array radiators, in which the parasitic elements were controlled by reactances. The Harrington antenna consisted of a central dipole surrounded by a ring of six dipoles loaded with parasitic reactive loads [4]. The next breakthrough in this field came with the appearance of ESPAR antennas, a project developed by Gyoda and Ohira in ATR laboratories in Japan in 2000. These antennas are a modified version of the original model Harrington, but used monopoles instead of dipoles, and reactive loads were integrated in the ground plane [3].

The printed Yagi-Uda antenna with electronic components and the ESPAR antenna can be included in the category of smart antennas, since both include electronic components for changing the radiation characteristics of the basic configuration of the antennas.

C. Operation principles

The operation of these antennas is based on the mutual coupling of the elements that constitute it. The monopoles are at a distance of approximately $\lambda/4$ from the active element [5]. The current in the active element induces currents on the passive elements. The amplitude and phase of the currents in parasitic elements will depend on the spacing between the elements and the dimensions of the dipoles aswell as the reactances applied to the parasitic dipoles, which corresponds to changing the electrical length of those elements [6].

D. Recent applications

Smart antennas have several applications in current systems that can be divided into three categories: Single Input, Multiple Output (SIMO), the Multiple Input, Single Output (MISO) and Multiple Input, Multiple Output (MIMO) [7].

These have an important role in today's wireless networks and systems. The antenna with multiple elements is used to increase the spectral efficiency, gain and decrease multipath spread [8].

Studies of milimeter waves wireless communication systems, are leading to the development of such technologies as gigabit Wireless Local Area Network (WLAN), automotive collision-avoidance and autonomous navigation radar systems [9]. The use of ESPAR antenna on mobile phones and personal computers and WLAN, has high potential [7]. These have been used for screening of base stations, satellite steering control and for use in vehicles.

Its characteristics allow its use in digital television receivers with diversity, Direction of Arrival (DoA) finders and applications in which adaptive radiation patterns are required.

It should be noted that smart antennas have numerous applications such as networking and wireless communication systems in civil, military or environments [10][11].

III. A SIMPLE DIPOLE MODEL

The Yagi-Uda antenna, as well as the ESPAR antenna, has parasitic elements that, in an axis of symmetry, can be modelled by an array of three dipoles.

The configuration of the ESPAR antenna can be used either with dipoles without a ground plane, or with monopoles on a ground plane. The study of the behaviour of parasitic elements in the radiation pattern is done with the addition of three elements. This array consists of three dipoles aligned along the x-axis, as can be seen in Figure 3.

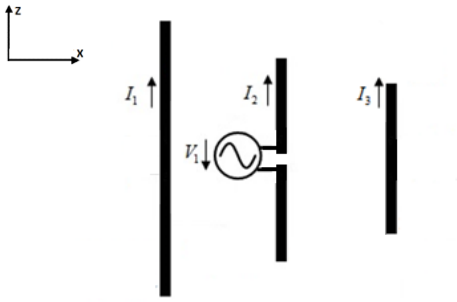

Fig. 3 –Three elements array

The complex amplitudes of the electric fields are [6]:

$$\bar{E}_{\theta_1} = j\frac{Z_0}{2\lambda r_1} I_1 h_{e_1} f_{D_1}(\theta) e^{-jkr_1} \qquad (1)$$

$$\bar{E}_{\theta_2} = j\frac{Z_0}{2\lambda r_2} I_2 h_{e_2} f_{D_2}(\theta) e^{-jkr_2} \qquad (2)$$

$$\bar{E}_{\theta_3} = j\frac{Z_0}{2\lambda r_3} I_3 h_{e_3} f_{D_3}(\theta) e^{-jkr_3} \qquad (3)$$

where:

Z_0 is the characteristic impedance in free space;

λ is the wavelength;

r_1, r_2, r_3 are the distance from the antenna to the reference point;

$h_{e_1}, h_{e_2}, h_{e_3}$ are the effective lengths of the antennas;

$f_{D_1}, f_{D_2}, f_{D_3}$ are the directional factors of the antennas;

θ is the position angle;

k is the propagation constant.

The complex amplitude of the total electric field is obtained from the equation [12]:

$$\begin{aligned} \bar{E}_{\theta_T} &= \bar{E}_{\theta_1} + \bar{E}_{\theta_2} + \bar{E}_{\theta_3} \\ \bar{E}_{\theta_T} &= \bar{E}_{\theta_2} \underbrace{\left(\frac{h_{e1}}{h_{e2}} \frac{\bar{I}_1}{\bar{I}_2} e^{jkd\cos\psi} + 1 + \frac{h_{e2}}{h_{e3}} \frac{\bar{I}_3}{\bar{I}_2} e^{jkd\cos\psi} \right)}_{\text{Array factor, } \bar{F}} \end{aligned} \qquad (4)$$

The calculation of the absolute value of the total electric field is obtained by the product of the magnitude of the electric field of the active antenna and the absolute value of the array factor [13].

$$|E_{\theta_T}| = |E_{\theta_2}(\theta)| * |\bar{F}| \quad (5)$$

The factors that influence the direction of the radiation pattern are the directional factor of the active antenna and the space factor of the array.

$$DR = |f_{D_2}(\theta)| * |\bar{F}| \quad (6)$$

Using the simulation program, the radiation pattern of the array of three elements, is shown in Fig. 4.

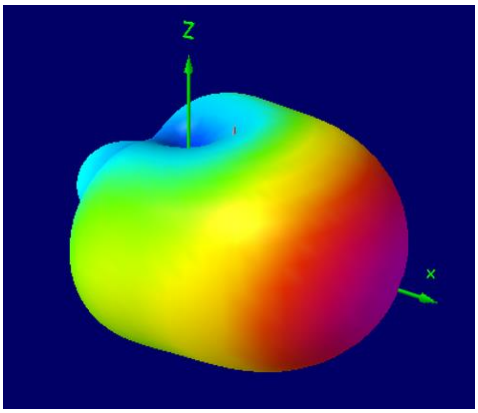

Fig. 4 – 3D radiation pattern of the 3 dipole arrays

Figure 4 shows that the radiation diagram presents a radiation maximum in the positive direction of the x-axis.

IV. Design and Optimization

A. Genetic algorithm

The antenna optimization algorithms allow to improve their radiation characteristics. This optimization technique is based on the principles of genetics and natural selection of Charles Darwin on the evolution of species and are designed by Genetic Algorithms (Gas) [14]. The Gas area powerfull tool which allows to handle multiple variables simultaneously.

In the case of ESPAR antenna, there are several variables that must be optimized. The number of variables increases with the number of parasitic antenna elements.

To apply the genetic algorithm to a ESPAR antenna is necessary to associate the antenna to an individual. Each antenna is evaluated and after evaluation is assigned a fitness value. This value is responsible for selecting the antennas to participate in the genetic operations. In each iteration performed, a new generation of antennas appears that will replace the previous generation, if they show better or improved features [15]. Otherwise the previous generation remains.

The antenna optimization cycle ends when several generations converge on the same solution, or if there is not a considerable improvement any longer.

B. Basic structure optimization

The optimization procedure is divided into three parts, structure optimizing, reactance optimization and design of the ground plane. In ESPAR antenna, the greater the number of parasitic elements, the greater the complexity. We have chosen to study an built an ESPAR antenna with 6 elements, because there is a good relationship between their performance and complexity. The radius of the monopole is 0.75 mm. The elements are arranged in a regular pentagon around the active element, as presented in (Figure 2).

C. Reactance optimization

For the reactances optimization, a variable reactance was placed at the base of each parasitic element. Changing the value of each reactance gives a variable radiation diagram, which is controlled through the five voltages applied V_m, $(m = 1, 2, 3, 4, 5)$. Figure 5 presents the electric scheme that ensures the variation of the reactance in each monopole. The variation is possible through the use of a pair of *varicap* diodes BB833 positioned in parallel at the termination of the parasitic element. In order to ensure the decoupling between the continuous voltage source signal and the RF signal on the monopole, a resistance is inserted R_1=10kΩ in series and a capacitor C_1= 3pF is inserted in parallel with the voltage source.

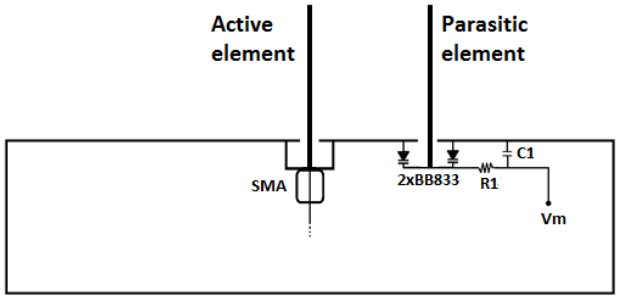

Fig. 5 – Electrical scheme applied to each monopole

According to the specifications of BB833 diode, the value of the capacity may vary from 0.9 pF to 9.3 pF, for a voltage up 30V. The configuration presented provides a variation of the reactance between -36.8j Ω and -3.5j Ω for a 2.4 GHz frequency. To enable a positive and negative change is necessary to make a shift to 20.2j Ω presented reactance range [16]. The displacement gives a reactance range -16.6j Ω the 16.6j Ω.

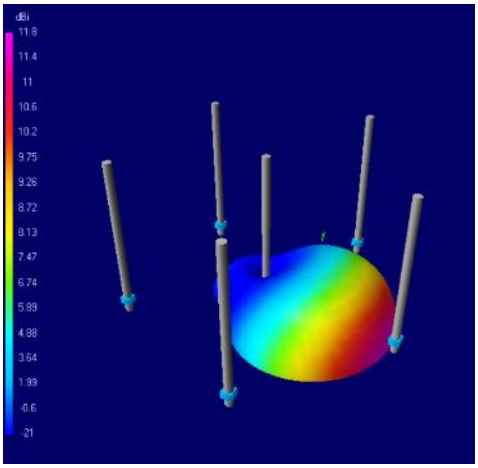

Fig. 6 - 3D radiation pattern

For the situation shown above (Fig. 6), the reactances associated with each parasitic monopole are shown in table I. The table

values are within the maximum and minimum of the range of values obtained by voltage variation applied to the varicap diodes.

Table I - Values of reactance

Reactive loads	Value ($j\boldsymbol{X_a}$)
X_1	-16
X_2	-16
X_3	16
X_4	16
X_5	-16

If inverted the reactance presented in table I, the 3D radiation pattern shown in figure 7 is obtained.

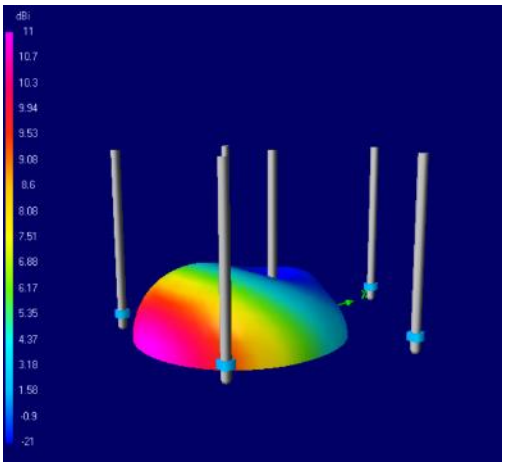

Fig. 7 - 3D radiation pattern

D. Ground Plane

The ground plane is of fundamental importance for the performance of the ESPAR antenna. From the previously optimized antenna with a conductive perfect ground plane, simulated previously, a new configuration was achieved by replacing the perfect conductor by, a circular copper ground plane, with radius 6.25 cm corresponding to 0.5λ. Figure 8 shows the 3D radiation pattern obtained for the simulation performed.

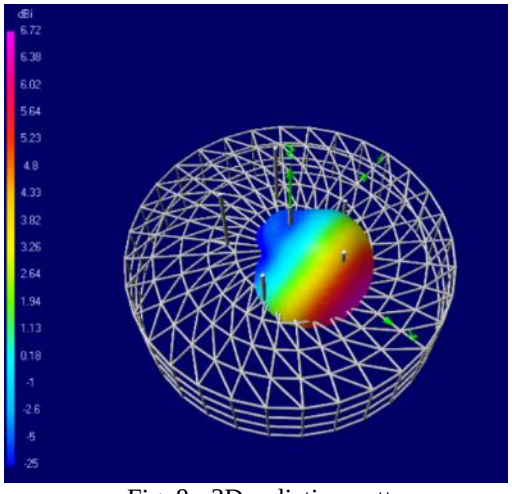

Fig. 8 - 3D radiation pattern

The use of the ground plane with flap ensures a mechanically suitable solution for the control mechanism and protection of the electronic elements.

The table II presents the final dimensions obtained for the antenna ESPAR of 6 elements.

Table II - Optimized values of variables

Variables	Value
Number of elements (N_e)	6
Diameter of monopoles (d_m)	1.5 mm
Ground plane ray (r_g)	6.2 cm
Distance between elements (r_p)	2.4 cm
Monopoles height (h_m)	2.8 cm
Flap height (h_s)	3.1 cm

V. Antenna ESPAR of 6 elements

A. Antenna design

Previous to the antenna construction a similar antenna according to the dimensions presented on the table II was designed.

This drawing was done using AutoCAD 2016, a tool that allows the antenna design in three dimensions. Figure 9 shows the top view of the design for the ESPAR antenna of 6 elements.

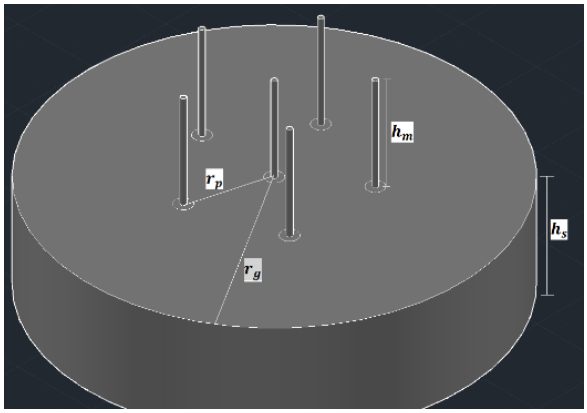

Fig. 9 - Top three dimensional view of the antenna building

B. Basic structure

In the construction of the basic structure was necessary a copper plate with a thickness 0.5 mm. Which was used to build the ground plane and the flap, which were welded together. After that, holes were made in the ground plane to place the monopoles. In order to fix and ensure the immobility of these run pipes were welded under the ground plane with the dimensions of the holes.

Figure 10 shows the antenna ESPAR after construction of the basic structure. The figure also shows the monopoles on the ground plane copper. At its base, the monopoles are surrounded by teflon to avoid electrical contact between them and the ground plane.

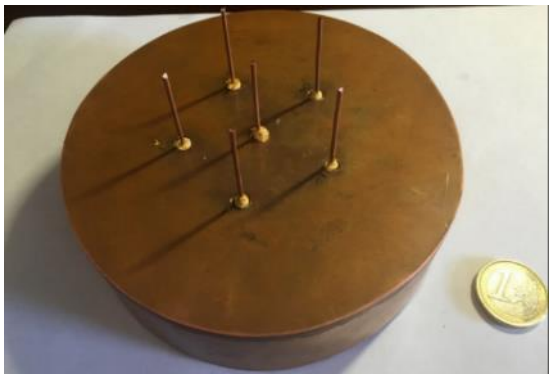

Fig. 10 – Photography ESPAR antenna basic structure

C. *Inclusion of electronic components*

The inclusion of the electronic components was based on the circuit of figure 5. Figure 11 shows the circuit associated with each of the monopoles. SMA (SubMiniature version A) plug was welded under active monopole and the existing brass tubes in the picture guarantee the stability of monopoles.

Fig. 11 - Electrical components associated with monopoles

The electrical components are connected to a printed circuit board. This was fastened to a styrofoam plate, also used to protect electronic components. Figure 12 shows the printed circuit board and styrofoam plate.

Fig. 12 - Fastened printed circuit board the styrofoam plate

D. *Antenna control*

For controlling voltages applied to the varicap diodes, it a control device was designed. This device is composed by several potentiometers in series, one for each monopole that allows to vary the applied voltage from 0V up to the maximum provided by the generator. To verify voltage is used alveoli. These are shown in figure 13 with blue and black color. Figure 13 shows the image of the control system after its construction.

Fig. 13 – Control device parasitic monopoles

VI. EXPERIMENTAL RESULTS

The validity of the values obtained in the simulation can only be proven by the experimental results.

A. *Antenna Impedance*

To make the ESPAR antenna impedance measurement a network analyser, from Agilent Technologies was used. This device is located in the radiofrequency (RF) laboratory 2 of the Telecommunications Institute (TI). The impedance of the antenna is given by $Z_L = R_a + jX_a$. It was obtained for the frequency of 2.4 GHz an impedance of $R_a = 55.8\,\Omega$ and a capacitive reactance $X_a = -32.4j\,\Omega$. Figure 14 shows the antenna impedance curve in Smith Char.

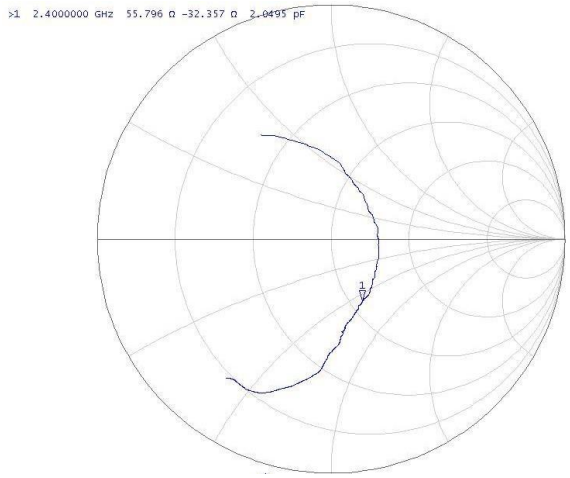

Fig. 14 - Antenna impedance curve in Smith Chart

B. S_{11} *parameter*

The implementation of measures $|S_{11}|_{dB}$ is subsequent to measuring the impedance of the ESPAR antenna. To perform the measurements again the network analyser had to be used. It performed the scanning frequency from 2 to 3 GHz.
Figure 15 shows a graph of variation of the S_{11}module as a function of frequency scan from 2 GHz to 3 GHz.

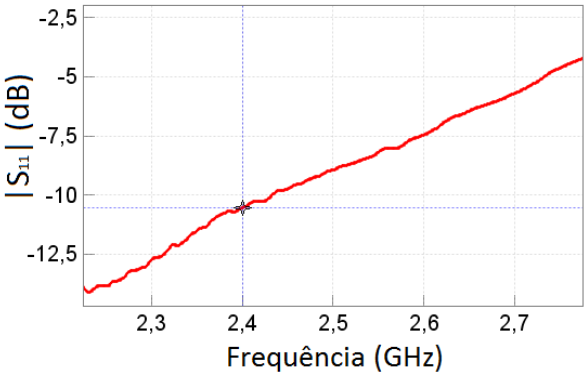

Fig. 15 - Parameter scattering matrix S_{11}

It is found that a value $|S_{11}|_{dB}$ = -10.54, for the frequency of 2.4 GHz, was obtained which is in accordance with the conditions of impedance matching, $|S_{11}|_{dB} \leq$ -10 [17].

C. *Radiation diagrams*

The experimental measurements of radiation patterns in the E and H planes were performed on the anechoic chamber of the Scientific Area of Electrical Engineering Department of Telecommunications and Computers (DEEC) from IST (Instituto Superior Técnico). This environment allows you to control the effects of fading by multipath. The chamber walls are lined with foam elements covered with graphite, to ensure absorption of the signals that reach the walls.

1) *Maximum foward the monopoles*

The following radiation diagrams show the comparison of measurements performed without applying voltage to the parasitic monopoles, blue curve, and with applying voltage with the combination of voltages 20V, 20V, 20V, 1V, 1V (red curve). The figure 16 shows the radiation pattern in the E plane and for these two settings.

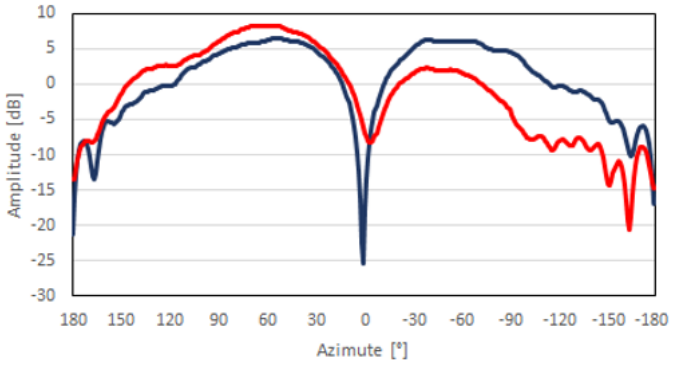

Fig. 16 - Radiation pattern E plane

From the analysis of the radiation pattern in the plane E, can be verified that the red curve has a well-defined maximum of radiation at 57° with the amplitude 8.3 dBi. The maximum represents the direction of the main lobe. The red curve represents a larger amplitude than the blue curve in the positive azimuth region, on the other hand, in the negative azimuth region the amplitude of the red curve is lower than the blue one.

Figure 17 shows the radiation diagram in the H plane for both configurations.

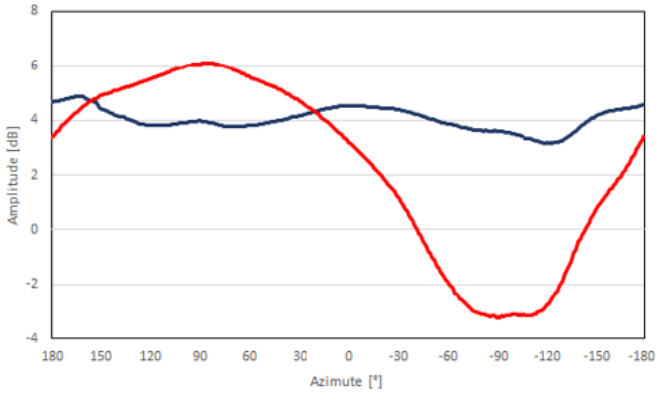

Fig. 17 - Radiation pattern H plane

From the analysis of the radiation diagram in the plane H, it can be seen that the red curve shows that the positive azimuth zone presents a greater amplitude than the negative radiation azimuth zone. The existence of a maximum in the red curve is visible in the 86° azimuth with the value of 6.1 dBi. The minimum occurs in azimuth and -90° with the amplitude value -3.23 dBi.
The analysis performed show a radiation pattern with no directive characteristics, which means that the radiation is not directed to a preferred site, location, as expected. In the second configuration a radiation diagram with directive characteristics is obtained.

2) *Maximum toward the bisecting of monopoles*

The following radiation diagrams show the comparison of measurements taken in the previous section (blue curve), when the combination 20V, 20V, 20V, 1V, 1V, was applied to the antenna and the section presented in this chapter (red curve), when applied the combination 1V, 1V, 1V, 20V, 20V.
The Figure 18 shows the radiation pattern in the E plane and for the two settings.

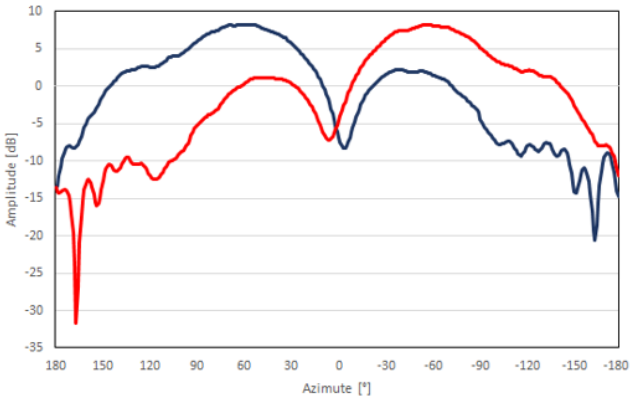

Fig. 18 - Radiation pattern E plane

The analysis of the radiation pattern in the plane E, verifies that the red curve shows a maximum radiation at -57°, with 8.2 dBi amplitude. This is opposite to what is observed in the blue curve. Note that the combination used in the previous section

has the maximum occuring at 57° and the amplitude obtained is substantially similar to the measurement performed.
Figure 19 shows the radiation diagram in the plane H for both configurations.

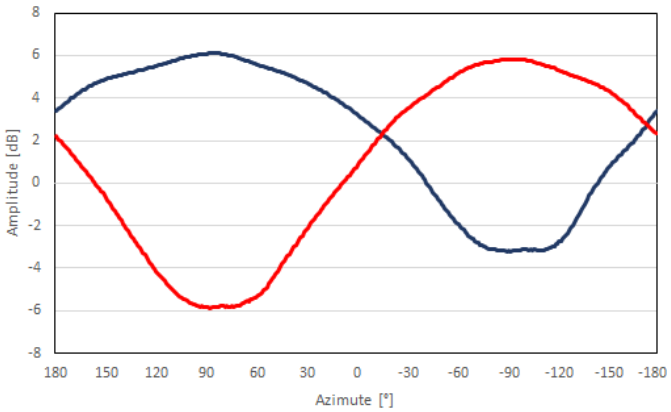

Fig. 19 - Radiation pattern H plane

From the analysis of the radiation diagram in the plane H, it can be seen that the red curve shows that the positive azimuth zone has lower amplitude radiation compared to the negative azimuth zone. The existence of a maximum in the red curve is visible in the azimuth -94°, the value of 5.82 dBi. The minimum occurs at azimuth 87° and the amplitude value is -5.86 dBi. The red curve shows higher amplitude than the blue curve in azimuth between -16° and -174°. The existence of a maximum in the red curve coincides with the minimum curve in blue, as required. The same is true when a minimum occurs in the red curve, there is a maximum in the blue curve. The influence of monopoles when reactive loads are reversed, as verified in simulation, was confirmed by the measurements.
After careful analysis of the experimental results with and without voltages applied to the parasitic monopoles, we came to the conclusion that the measurement results are consistent with the simulations performed.

VII. Conclusions

This master thesis has as main purpose the comparative study of two antennas for communication in 2.4 GHz. Figure 20 shows the printed Yagi-Uda antenna.

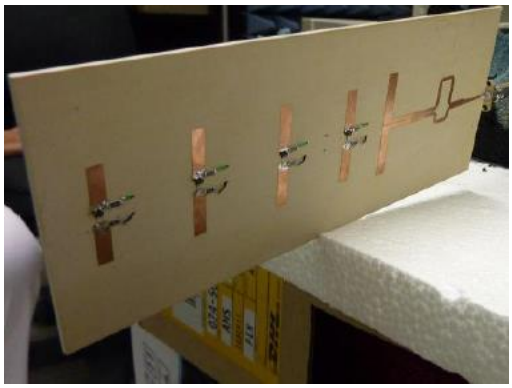

Fig. 20 – Printed Yagi-Uda antenna [18]

The printed Yagi-Uda antenna and ESPAR antenna can be included in the category of smart antennas. These two shows antenna construction projects for communication with the Robots developed by the Portuguese Army.
The printed Yagi-Uda antenna, a prototype developed in a previous dissertation, has as a main radiation characteristic the possibility of allowing a high gain and control of the Half-power beamwidth (HPBW). To accomplish the switching, PIN diodes are used, placed between two "arms" of directors elements [18]. With the increase of the number of short circuit diodes, the HPBW decreases and the gain increases.
This Yagi-Uda antenna aimed at change the width of the main lobe radiation pattern. If the main lobe is wider, it is possible for the antenna to communicate with two robots, but if the main lobe is narrow the antenna only communicates with one robot.
The prototype of the ESPAR antenna aimed at switching the radiation pattern in azimuth. This capability allows to communicate with a moving robot, keeping the antenna unmoved.
The proposed objectives were acquired. The results obtained in experimental measurements are consistent with the simulations performed and are in accordance with other results in the existing literature.

VIII. Conclusion

During the course of this work skills in the design, simulation antenna construction were acquired. This project has proved to be multivalent, since in addition to the performed simulations with focus on the development of the prototype, also allowed to acquire practical skills in performing the same.

References

[1] U.S. Department of Defence, “Unmanned Systems Integrated Roadmap,” 2013.
[2] S. J. Orfanidis, Electromagnetic Waves and Antennas, New Jersey: Rutgers University, 2008.
[3] A. Kalis, A. Kanatas e C. Papadias, Parasitic Antenna Arrays for Wireless MIMO Systems, Springer, 2014. ISBN 978-1-4614-7998-7. Cap.1 e 2.
[4] R. F. Harrington, "Reactively Controlled Directive Arrays, " IEEE - Transactions on Antennas and Propagation, vol 26 no.3, pp 390-395, Maio 1978.
[5] H. Kawakami and T. Ohira, “Electrically Steerable Passive Array Radiator (ESPAR) Antennas,” IEEE - Transactions on Antennas and Propagation, Vol 47 no. 2, pp. 43–49, 2005.
[6] M. J. Martins e I. V. Neves, Propagação e Radiação de Ondas Eletromagnéticas, Lisboa: LIDEL. ISBN 2015,978-989-752-066-2. Cap. 7 e 8.
[7] A. Kausar, M. A. Cheema, S. Kausar, H. Rehman e T. Hassan, “ESPAR Antenna System Designing & Simulation" em First International Conference on Systems Informatics, 2014.
[8] R. Schlub, J. Lu, and T. Ohira, “Seven-Element Ground Skirt Monopole ESPAR Antenna Design from a Genetic Algorithm and the Finite Element Method,” IEEE - Transactions on Antennas and Propagation, vol. 51, no. 11, pp. 3033–3039, 2003.
[9] B. K. Tehrani, B. S. Cook e M. M. Tentzeris, “Inkjet Printing of Multilayer Millimeter-Wave Yagi-Uda Antennas on Flexible Substrates,” IEEE ANTENNAS AND WIRELESS PROPAGATION LETTERS, vol. x, no. x, May 2015.
[10] S. A. Mitilineos, K. S. Mougiakos, and S. C. A. Thomopoulos, “Design and Optimization of ESPAR Antennas via Impedance Measurements and

a Genetic Algorithm," IEEE Antennas Propag. Mag., vol. 51, no. 2, pp. 118–123, 2009.
[11] J. M. Berger, Tese de Mestrado - "Low Cost Direction Finding with the Electronically Steerable Parasitic Array Radiator (ESPAR) Antenna," University of the Witwatersrand, Johannesburg, 2005.
[12] C. A. Balanis, Antenna Theory Analysis and Design, New Jersey: John Wiley & Sons, 2005.
[13] A. A. Silva, Tese de Mestrado - "Modificação das Caraterísticas de Radiação de uma Antena usando Componentes Eletrónicos", Lisboa, Instituto Superior Técnico, 2015.
[14] R. L. Haupt, S. E. Haupt, Pratical Genetic Algorithms- Second Edition, New Jersey: John wiley & Sons, 2004.
[15] Y. Kuwahara, "Multiobjective Optimization Design of Yagi-Uda Antenna," IEEE Transactions on Antennas and Propagation, Vol. 53, No. 6, pp. 1984–1992, June 2005.
[16] C. Sun, S. Member, A. Hirata, T. Ohira, N. C. Karmakar, and S. Member, "Fast Beamforming of Electronically Steerable Parasitic Array Radiator Antennas : Theory and Experiment," IEEE - Transactions on Antennas and Propagation, vol. 52, no. 7, pp. 1819–1832, 2004.
[17] E. Palantei, "Switched Parasitic Smart Antenna : Design and Implementation for Wireless Communication Systems," no. May, 2008.
[18] T. Daniel and S. De Almeida, "Projecto de uma Antena para Comunicação Wireless do ROVIM Tiago Daniel Sanches de Almeida Engenharia Electrotécnica e de Computadores Júri," 2013.

Edgar Ruano was born in Miranda do Douro, Portugal, on November 15, 1991. In 2010 he joined the Portuguese Army where he completed the "licenciatura" in Telecomunications at the Military Academy, in Lisbon. At the same time, he is a Master Student in Electrical and Computer Engineering Master course at Instituto Superior Técnico, Lisbon.